sciendo
Journal of ELECTRICAL ENGINEERING, VOL 69 (2018), NO5, 390–394

Channel temperature analysis of AlGaN/GaN HEMTs in quasi-static and pulse operation mode

Martin Florovič *, **Róbert Szobolovszký** *, **Jaroslav Kováč, Jr.** *, **Jaroslav Kováč** *, **Aleš Chvála** *, **Jean-Claude Jacquet** **, **Sylvain Laurent Delage** **

GaN-based HEMTs' high potential is deteriorated by self-heating during the operation, this has influence on the electrical properties as well as device reliability. This work is focused on an average channel temperature determination of power AlGaN/GaN HEMT prepared on SiC substrate using quasi-static and pulsed I-V characterization. There was analyzed the drain current change relation to temperature dependent electrical HEMT parameters such as source resistance, threshold voltage, saturation velocity, resp. leakage current which allows to calculate an average channel temperature versus dissipated power for various ambient temperature. Differential temperature of investigated device with and without heatsink was determined. Obtained results were discussed using simulated spatial temperature distribution.

K e y w o r d s: high-electron-mobility transistor (HEMT), AlGaN/GaN

1 Introduction

The advanced GaN-based devices are promising to use for high temperature, frequency, power and microwave applications. In fact, a high potential of these devices is deteriorated by self-heating during the HEMT operation, this has influence on the electrical characteristics as well as device reliability [1-3], temperature is one of the dominant factor here. A high thermal conductance of particular materials, especially substrate, plays significant role in the power heat transfer. Power devices prepared on SiC and Si substrates exhibits better power dissipation than the ones grown on sapphire substrate [4].

Various experimental methods essential for complex characterization were developed to determine indirectly channel temperature of GaN-based HEMTs, *eg* Raman spectroscopy or interferometric mapping [5-7]. These techniques are widely applied but some of them require advanced setup to obtain accurate results. In some cases special test structures or support measurements are needed. In symbiosis with thermal simulations experimental data can help to understand thermal processes inside the structure.

In this work an adapted method [8] was utilized for and the consecutive analysis to determine the channel temperature of HEMT is presented. This method can be easily applied directly on any device layout down to submicron dimensions. The method can be also used on different structures to investigate the role of the particular transistor elements, eg. gate, gap dimensions or material composition.

2 Theory

The approximate drain current I_D difference in the operating point (drain V_{DS} and gate V_{GS} voltage) in the saturation regime of HEMT is given mainly by the voltage drop caused by the source resistance R_S, threshold voltage V_{TH} variation multiplied by transconductance g_m of investigated HEMT, leakage current variation $\mathrm{d}I_L$ with temperature [9,10] and additional current variation $\mathrm{d}I_{DA}$ caused by electric field and temperature change in the active area. Based on [8] differential form of the drain current change can be written as

$$\mathrm{d}I_D = -g_m I_D \mathrm{d}R_S - g_m \mathrm{d}(V_{TH}) + \mathrm{d}I_L + \mathrm{d}I_{DA} \qquad (1)$$

The total resistance R_{DS} is given by source and drain contact resistance R_C, source to gate channel resistance R_{GS} (in the length d_{GS}), drain to gate channel resistance R_{GD} (in the length d_{GD}) and gate channel resistance R_G (in the length d_G)

$$R_{DS} = R_{GS} + R_{GD} + R_G + 2R_C \qquad (2)$$

There is a constant specific resistance in neutral channel areas between gate and source/drain $R_{GS}/\mathrm{d}_{GS} = R_{GD}/\mathrm{d}_{GD}$ [11] and therefore

$$R_S = R_{GS} + R_C = \\ = \frac{(R_{DS} - R_G)\mathrm{d}_{GS} + R_C(\mathrm{d}_{GS} - \mathrm{d}_{GD})}{\mathrm{d}_{GS} + \mathrm{d}_{GD}} \qquad (3)$$

* Institute of Electronics and Photonics, Faculty of Electrical Engineering and Information Technology, Slovak University of Technology, Ilkovičova 3, 812 19 Bratislava, Slovakia, martin.florovic@stuba.sk, ** III-V Lab, route de Nozay, 91460 Marcoussis, France

DOI: 10.2478/jee-2018–0057, Print (till 2015) ISSN 1335-3632, On-line ISSN 1339-309X © 2018FEI STU

Temperature dependence of R_S should be obtained from linear regime of output characteristics where self-heating and trapping (low V_{DS} and short pulse measurements) could be neglected. For $V_{DS} << V_{GS} - V_{TH}$ potential difference across the channel affects slightly vertical electric field under the gate and R_G is given

$$R_G = -\frac{(R_D S - 2R_C)V_{TH}\mathrm{d}_G}{(V_{GS} - V_{TH})(\mathrm{d}_{GS} + \mathrm{d}_G + d_{GD})} \tag{4}$$

Equations (3) and (4) allow calculation of R_S at particular temperature.

Temperature dependence of V_{TH} is connected with the sheet carrier concentration and the built-in Schottky gate potential [12,13] such as trap generation nearby gate. Those traps influence vertical electric field under the gate which results in I_D time change depending on trapped charge [14,15]. Assuming that traps are mostly filled by free carriers from the 2DEG channel for V_{GS} lower than built-in Schottky gate potential V_{GS} resp. V_{DS} timing result in the same I_D . V_{TH} such as I_L should be determined from transfer $I-V$ characteristics for HEMT operating in low power regime (V_{GS} nearby V_{TH}). If above mentioned dependence exhibits $\Delta V_{TH} << V_{GS} - V_{TH}$ or $V_{GS} \to 0$ V R_S could be get directly from quasi-static measurements.

In practical applications the most appropriate way is to get I_D, g_m (output $I-V$ characteristics in saturation regime) and R_S, V_{TH} (output and transfer $I-V$ characteristics in low power regime) at the same transient conditions. Drain current I_{D0}, or transconductance g_{m0} at the reference temperature T_0 are needed as input parameters. If $\mathrm{d}I_{ND}$ in (1) is temperature independent it could be included in I_{D0}. Polynomial fit of $\mathrm{R}_S(\mathrm{T})$, $\mathrm{V}_{TH}(\mathrm{T})$, $\mathrm{I}_L(\mathrm{T})$ with $\mathrm{g}_m(\mathrm{T})$ estimation and integration of (1) should be used to determine temperature at the operating point set by V_{GS} and V_{DS}. There is usually used the same temperature for V_{TH}, R_S and I_L in above mentioned fitting, this is medium value in the device in spite of thermal gradients above $\approx 20\,^\circ\mathrm{C}/\mu\mathrm{m}$ nearby gate in such power devices [16]. First term (R_S) in (1) reflects the average temperature in the source - gate area whereas second one (V_{TH}) in the active area under the gate and third one ($\mathrm{d}I_L$) nearby the device surface. Actually g_m is associated with the parameters in active and neutral area [17].

I_{D0} and g_{m0} can be determined from short-pulse measurements ($\approx$ 10 ns) with negligible self-heating for $\Delta \mathrm{V}_{TH} << V_{GS} - \mathrm{V}_{TH}$. There is also a way of polynomial I_D, g_m extrapolation for pulsed output $I-V$ characteristics in saturation regime which allows to estimate I_{D0} and g_{m0} (theoretical non-self-heating values), this estimation can be used as well for static operation.

The above method should be simplified for practical purposes. Following average values should be defined

$$\overline{g_m} = \frac{g_m + g_m 0}{2}, \quad \overline{I_D} = \frac{I_D + I_{D0}}{2} \tag{5}$$

For relative small change of I_D and g_m the equation (4) using equations (8) can be transformed to the difference form

$$\begin{aligned}\Delta I_D &= I_D - I_{D0} = \\ &= \Delta I_L + \Delta I_{DA} - \overline{g_m}\left[\overline{I_D}\Delta R_S + \Delta V_{TH}\right]\end{aligned} \tag{6}$$

Linearization of $V_{TH}(T)$, $\mathrm{R}_S(\mathrm{T})$, resp. $\mathrm{I}_L(\mathrm{T})$ allows to obtain the temperature change by solving linear equation (9). Advanced fabricated GaN-based HEMTs exhibit small $\mathrm{d}I_{DA}$ in saturation regime due to low carrier concentration and saturation velocity change in the active channel area and minor leakage paths allow to neglect $\mathrm{d}I_L$.

If there is roughly estimated the channel temperature (in neutral, resp. active area) needed for parameter linearization there should be determined the differential temperature of investigated device without or with heatsink or fan, case 1 and 2

$$\overline{g_m} = \frac{g_{m1} + g_{m2}}{2}, \quad \overline{I_D} = \frac{I_{D1} + I_{D2}}{2} \tag{7}$$

$$\begin{aligned}\Delta I_D &= I_{D2} - I_{D1} = \\ &= \Delta I_L + \Delta I_{DA} - \overline{g_m}\left[\overline{I_D}\Delta R_S + \Delta V_{TH}\right]\end{aligned} \tag{8}$$

This can assist to design HEMT substrate or base plate. Rough temperature estimation, resp. linear R_S and V_{TH} temperature dependence for calculations in (8) is required, there is no need of I_{D0} and g_{m0} parameters, only I_D and g_m average values (7).

3 Experimental

The investigated AlGaN/GaN HEMT structure a 1.5 nm GaN-cap/ 14.5 nm $\mathrm{Al}_{0.29}\mathrm{GaN}$ -barrier/50 nm GaN-spacer /1.650 μm GaNdoped heterostructure grown on 500 μm 4H-SiC substrate. The backside 500 μm thick Au contact on substrate side of the transistor is soldered to the 1 mm thick CuMo leadframe by 25 μm thick AuSn solder. Top ohmic drain/source and gate contacts are created by Au metallization layers with thicknesses of 0.5 μm and 0.6 μm, respectively. The investigated HEMT is $\approx$125 μm wide with gate length $\approx$1.2 μ m and the same drain-gate and source-gate length $\approx$5 μ m. The structure is set in open package which was optionally placed on the Al heatsink preserved at constant temperature.

The output and transfer $I-V$ characteristics were measured using semiconductor parameter analyzer Agilent 4155C and regulated heat-flow oven. To obtain change in output $I-V$ characteristics caused by self-heating the gate voltage V_{GS} was kept at 0 V, while the drain voltage V_{DS} was varied from 0 V up to 40 V. Source resistance R_S and threshold voltage V_{TH} were obtained from $I-V$ characteristics measured at ambient temperature range 25 – 120 °C in low power regime,

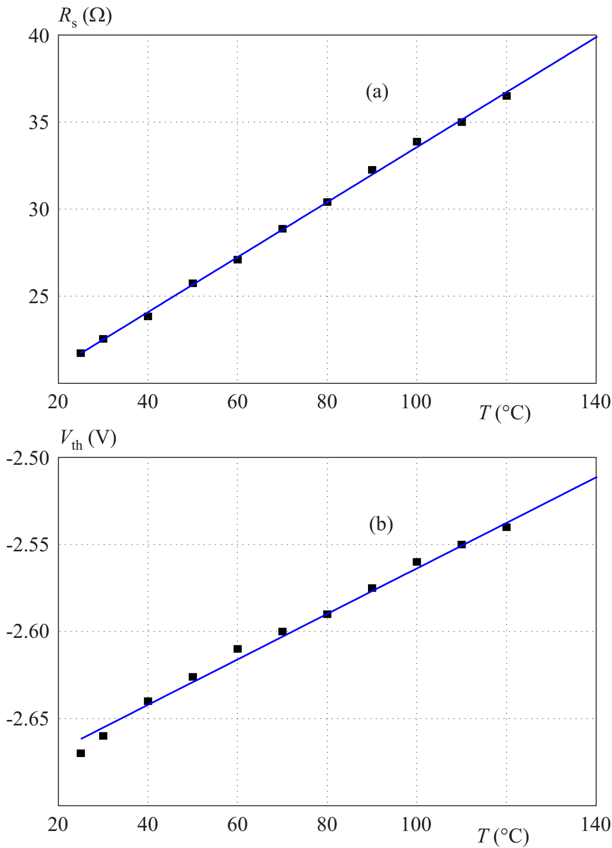

Fig. 1. (a) – source resistance R_S, (b) – threshold voltage V_{TH} temperature dependence for investigated sample

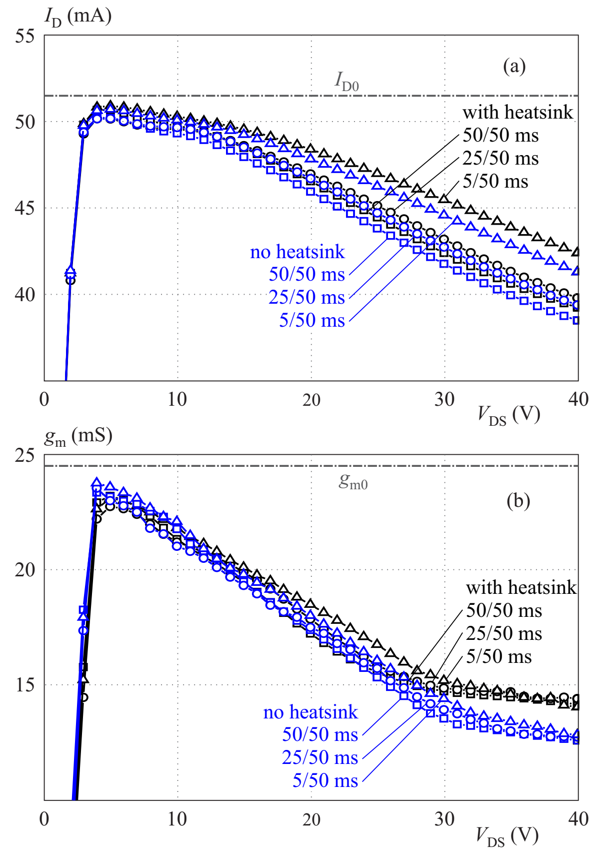

Fig. 2. (a)–output $I-V$ characteristics, (b) - transconductance of investigated sample

respectively. There was pulsed V_{DS} with pulse width of ≈5 ms, ≈25 ms (pulsed) and ≈50 ms (quasi-static) with period of ≈50 ms. White LED device state recovery was applied after each measurement for one minute at zero applied voltage.

Temperature dependence of R_S and V_{TH} obtained from static output and transfer $I-V$ characteristics are plotted in Fig. 1(a) and Fig. 1(b) respectively, linear extrapolation was used. In Fig. 2(a),(b) there are shown static output $I-V$ characteristics and calculated g_m measured at gate voltage $V_{GS} = 0$V at ambient room temperature. V_{DS} increase causes power dissipation resulting in self-heating and consecutive I_D and g_m decrease. Investigated sample exhibits $\Delta V_{TH} << I_D \Delta R_S$ which points on low sheet carrier concentration, Schottky contact barrier height and trap density variation with temperature in the investigated HEMT structure. Therefore there were found the same non-self-heating values $I_{D0} = 51.5$ mA, $g_{m0} = 24.5$ mS for quasi-static such as pulsed regime assuming small change with V_{DS}.

Using (5) and (6) an average channel temperature was calculated as shown in Fig. 3(a) from average I_D values during the pulse measured by employed parameter analyzer. Thermal resistance R_{TH} of the device shown in Fig. 3(b) is calculated from the temperature dependence slope in Fig. 3(a). Shorter pulse length, resp. longer cooling during pulse break, lower power and heatsink preserved at room temperature results in better power dissipation because of lower reached temperature during the pulse supported by thermal conduction of particular materials decrease with temperature. In the case of quasi-static measurements R_{TH} is close to the device thermal resistance used in thermal circuit model.

Spatial temperature distribution nearby the surface in the HEMT middle in DC operating state of investigated HEMT with heatsink preserved at constant temperature ≈ 25 °C shown in Fig. 4(a) was simulated and designed by Sentaurus Device Editor. Pinch-off area nearby gate-to-drain interface acts as the main heat source with highest power density. In ideal case the solution is combination of cylindric heat transfer equation (≈ $\ln r$, dominant nearby the HEMT active area in the device middle) and spherical heat transfer equation (≈ $1/r$, dominant in the remote area, respectively device edge). Real conditions such as the multilayered HEMT structure including the device air interface such as non-constant thermal conduction result in temperature profile deviation in comparison with solutions mentioned above. Whereas source-gate neutral area defined by R_{GS} produces ≈ 50 mW in HEMT saturation regime there is obvious temperature difference above 40 °C for power above ≈ 1.5 W across this area, thermal trapping dependence is low, there should be temperature in this range expected. However from quasi-static experiments, Fig. 2(a),(b) higher calculated temperature, Fig. 3(a) was obtained, this could be explained by following: g_m change is caused not only

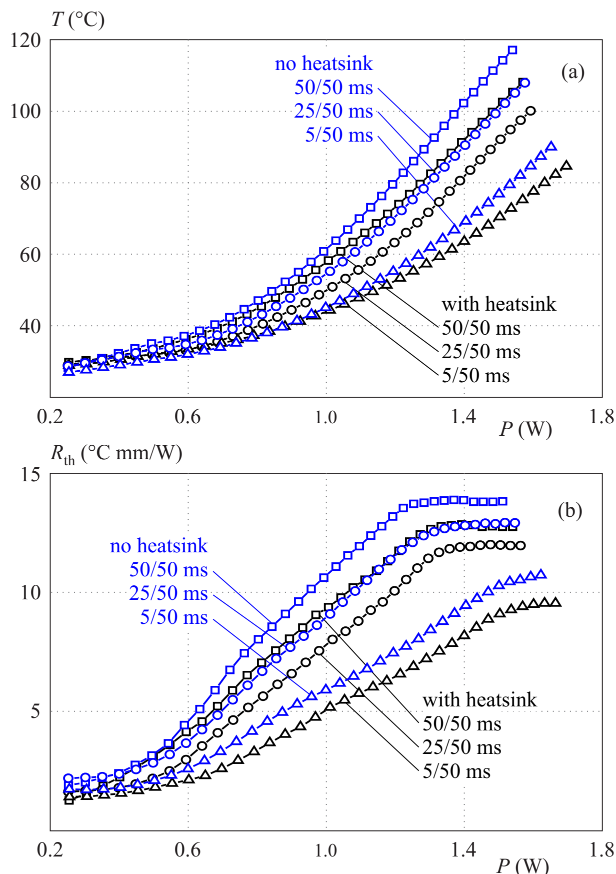

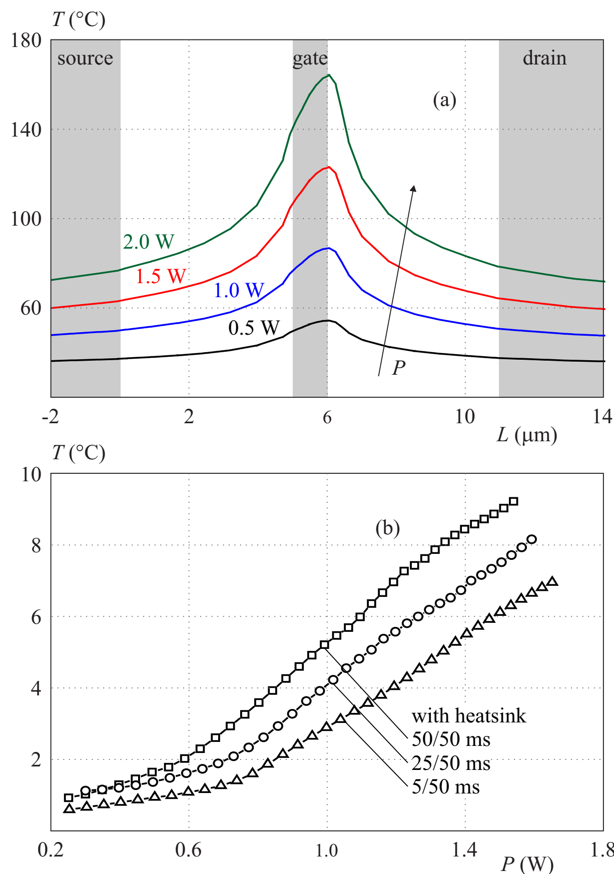

Fig. 3. (a)–average channel temperature,(b)–thermal resistance *vs* dissipated power for investigated sample

Fig. 4. (a)–channel temperature spatial distribution,(b)–channel temperature difference *vs* dissipated power for investigated sample

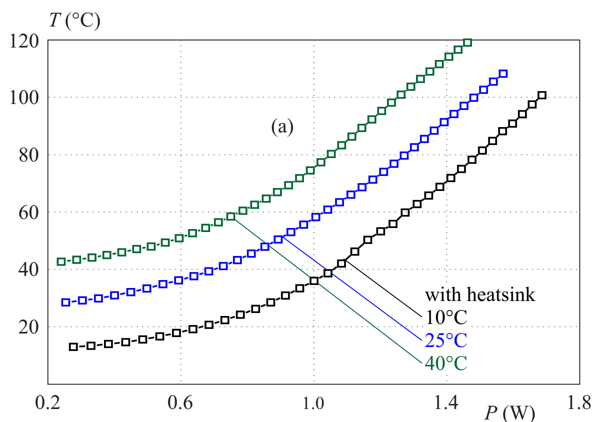

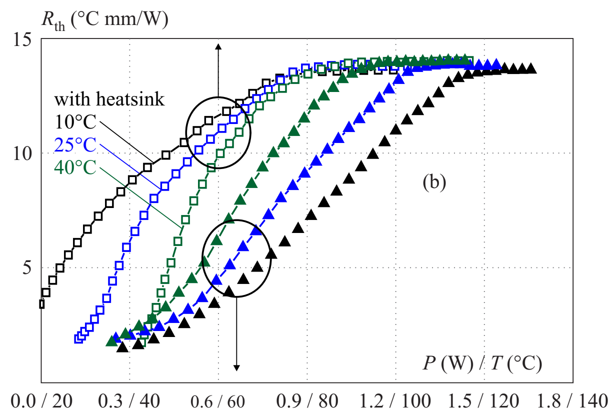

Fig. 5. (a)– channel temperature, (b) – thermal resistance *vs* dissipated power, respecxtively temperature for investigated sample at various ambient temperature

by the R_S variation but also by the thermal dependence of electron mobility, resp. saturation velocity, such as concentration in 2DEG. Vertical electric field under the gate, channel shortening, current collapse, resp. carrier mobility dependence on horizontal electric field plays role in I_{D0} and g_{m0} determination especially for higher applied V_{DS} . In general, if more thermal dependent device parameters affecting output values I_D and g_m in the same way are included in the model there is lower temperature calculated. Additionally, thermal capacity C_{TH} plays significant role in temperature time response. Heatsink attached to as large as possible area of the socket increases R_{TH} and C_{TH} . Inconsiderable role plays SiC substrate solder brass socket such as socket heatsink interface here.

4 Conclusions

Channel temperature *vs* dissipated power in a $Al_{0.29}Ga_{0.71}N/GaN$ HEMT in saturation regime was calculated for pulsed and quasi-static operation. Theoretical analysis of drain current change with temperature was discussed

with respect on the device parameters (transconductance, serial resistance, threshold voltage and velocity).

From quasi-static and pulsed measurements was calculated channel temperature from drain current difference equation (50/50 ms: $T = 108$ °C for $P = 1.55$ W, 25/50 ms: $T = 100$ °C for $P = 1.58$ W, 5/50 ms: $T = 85$ °C for $P = 1.64$ W, for device with heatsing attached). There was obtained differential temperature $\Delta T6 - 10$ °C for $P = 1.55$ W, to show the heatsink influence on channel temperature. Thermal resistance dependence was explained. Obtained channel temperature is average because of high thermal gradients in such HEMT devices as shown in simulated spatial temperature distribution.

Similar measurements were done for various ambient heatsink temperature (10 °C, 25 °Cand 40 °C). From calculations there is obvious that drain current and transconductance in saturation regime depends on distributed device parameters. In device operation under $\approx$ 0.5 W and also above $\approx$ 80 °Caverage channel temperature rises linearly.

This analysis described AlGaN/GaN HEMT thermal behavior for different operating conditions in practical way. Investigated sample exhibits low trap density across the HEMT structure. There is needed more comprehensive equipment, especially for short pulse measurements, to perform more accurate calculations covering associated effects as charge trapping, current collapse and thermal gradients across the investigated structure.

Acknowledgment

The research leading to these results has received funding from the Electronic Component Systems for European Leadership Joint Undertaking under grant agreement No 662322, project OSIRIS. This Joint Undertaking receives support from the European Unions Horizon 2020 research and innovation program, France, Norway, Slovakia and Sweden. This publication reflects only the author's view and the JU is not responsible for any use that may be made of the information it contains. The work was also supported by Grant VEGA 1/0491/15 through the Ministry of Education, Science, Research and Sport of Slovakia.

References

[1] [1] O. Ambacher, J. Smart, J. R. Shealy, N. G. Weimann, K. Chu, M. Murphy, W. J. Schaff, L. F. Eastman, R. Dimitrov, L. Wittmer, M. Stutzmann, W. Rieger and J. Hilsenbeck, "Two-dimensional electron gases induced by spontaneous and piezoelectric polarization charges in N- and Ga-face AlGaN/GaN heterostructures", *Journal of Appl. Phys.*, ol.85, no.6, pp.3222-3233, 1999.

[2] A. Nigam, T. N. Bhat, S. Rajamani, S. B. Dolmanan, S. Tripathy and M. Kumar, "Effect of self-heating on electrical characteristics of AlGaN/ GaN HEMT on Si (111) substrate", , *AIP Advances 7*, pp.85015, 2017.

[3] M. K. Chattopadhyay and S. Tokekar, "Thermal model for dc characteristics of Algan/Gan HEMTs including self-heating effect and non-linear polarization", *Microelectronics Journal*, 39, pp.1181-1188, 2008.

[4] S. Chowdhury, "Gallium nitride based power switches for next generation of power conversion", *Phys. Stat. Sol. (A)*, vol.212, iss.5, pp.1066-1074, 2015.

[5] F. Berthet, Y. Guhel, H. Gualous, B.Boudart, J.-L. Trolet, M. Piccione and C. Gaqui?re, "Characterization of the self-heating of AlGaN/GaN HEMTs during an electrical stress by using Raman spectroscopy", *Microel. Rel.*, vol.51, pp.1796-1800, 2011.

[6] J. Kim, J. A. Freitas, J. Mittereder, R. Fitch, B. S. Kang, S. J. Pearton and F. Ren, "Effective temperature measurements of AlGaN/GaN-based HEMT under various load lines using micro-Raman technique", *Solid-State Electr.*, vol.50, pp.408-411, 2006.

[7] Y. Li-Yuan, X. Xiao-Yong, Z. Kai, Z. Xue-Feng, M. Xiao-Hua and H. Yue, "Channel temperature determination of a multifinger AlGaN/GaN high electron mobility transistor using a micro-Raman technique", *Chinese Physics B*, vol.21, no.7, pp.077304-1-3, 2012.

[8] J. Kuzmik, P. Javorka, A. Alam, M. Marso, M. Heuken and P. Kordos, "Determination of Channel Temperature in AlGaN/GaN HEMTs Grown on Sapphire and Silicon Substrates Using DC Characterization Method", *IEEE Trans. Electr. Dev.*, vol.49, no.8, pp.1496-1498, 2002.

[9] S. Arulkumaran, T. Egawa, H. Ishikaw and T. Jimbo, "Temperature dependence of gate-leakage current in AlGaN/GaN high-electron-mobility transistors", , *App. Phys. Letters*, vol.82, no.18, pp.3110-3112, 2003.

[10] A. Mimouni, T. Fernndez, J. Rodriguez-Tellez, A. Tazon, H. Baudrand and M. Boussuis, "Gate Leakage Current in GaN HEMT's: A Degradation Modeling Approach", *Electrical and Electronic Engineering*, vol.2, no.6, pp.397-402, 2012.

[11] R. Menozzi, G. A. Umana-Membreno, B. D. Nener, G. Parish, G. Sozzi, L. Faraone and U. K. Mishra, "Temperature-Dependent Characterization of AlGaN/GaN HEMTs: Thermal and Source/ Drain Resistances", *IEEE Trans. Dev. and Mat. Rel.*, vol.8, no.2, pp.255-264, 2008.

[12] P. Das and D. Biswas, "Simplified 2DEG carrier concentration model for composite barrier AlGaN/GaN HEMT", *AIP Conf. Proc 1591*, pp.1449-1451, 2014.

[13] J.-H. Shin, J. Park, S.-Y. Jang, T. Jang and K. S. Kim, "Metal induced inhomogeneous Schottky barrier height in AlGaN/GaN Schottky diode", *Appl. Phys. Letters*, no.102, pp.243505, 2013.

[14] J. M. Tirado, J. L. Sanchez-Rojas and J. I. Izpura, "Trapping Effects in the Transient Response of AlGaN/GaN HEMT Devices", *IEEE Trans. Electr. Dev.*, vol.54, no.3, pp.410-417, 2007.

[15] M. Florovic, J. Skriniarova, J. Kovac and P. Kordos, "Trapping analysis on AlGaN/GaN Schottky barrier", *Semicond. Sci. Technol.*, vol.32, pp.025017, 2017.

[16] J. Joh, J. A. del Alamo, U. Chowdhury, T.-M. Chou, H.-Q. Tserng and J. L. Jimenez, "Measurement of Channel Temperature in GaN High-Electron Mobility Transistors", *IEEE Trans. Electr. Dev.*, vol.56, no.12, pp.2895-2901, 2009.

[17] B. Raj and S. Bindra, "Thermal Analysis of AlGaN/GaN HEMT: Measurement and Analytical Modeling Techniques", *Int. Journal of Comp. Apps. (0975 - 8887)*, vol.75, no.18, pp.4-13, 2013.

[18] J. Das, H. Oprins, H. Ji, A. Sarua, W. Ruythooren, J. Derluyn, M. Kuball, M. Germain and G. Borghs, "A Temperature Analysis of High-power AlGaN/GaN HEMTs", *THERMINIC 2006 Proc.*, pp.38-41, 2006.

Received 9 August 2018